frontiers in Ecology and Evolution

ORIGINAL RESEARCH
published: 05 August 2021
doi: 10.3389/fevo.2021.659039

# Modeling Sprawling Locomotion of the Stem Amniote *Orobates*: An Examination of Hindlimb Muscle Strains and Validation Using Extant *Caiman*

*Michelle Zwafing[1], Stephan Lautenschlager[2], Oliver E. Demuth[3,4] and John A. Nyakatura[1]**

*[1] Lehrstuhl für Vergleichende Zoologie, Institut für Biologie, Humboldt Universität zu Berlin, Berlin, Germany, [2] School of Geography, Earth and Environmental Sciences, University of Birmingham, Birmingham, United Kingdom, [3] Department of Earth Science, University of Cambridge, Cambridge, United Kingdom, [4] Structure and Motion Laboratory, Department of Comparative Biomedical Sciences, Royal Veterinary College, London, United Kingdom*

OPEN ACCESS

**Edited by:**
*Julia L. Molnar, New York Institute of Technology, United States*

**Reviewed by:**
*Stephanie E. Pierce, Harvard University, United States*
*Emanuel Andrada, Friedrich Schiller University Jena, Germany*

***Correspondence:**
*John A. Nyakatura*
*john.nyakatura@hu-berlin.de*

**Specialty section:**
*This article was submitted to Paleontology, a section of the journal Frontiers in Ecology and Evolution*

**Received:** *26 January 2021*
**Accepted:** *15 July 2021*
**Published:** *05 August 2021*

**Citation:**
*Zwafing M, Lautenschlager S, Demuth OE and Nyakatura JA (2021) Modeling Sprawling Locomotion of the Stem Amniote Orobates: An Examination of Hindlimb Muscle Strains and Validation Using Extant Caiman. Front. Ecol. Evol. 9:659039. doi: 10.3389/fevo.2021.659039*

The stem amniote *Orobates pabsti* has been reconstructed to be capable of relatively erect, balanced, and mechanically power-saving terrestrial locomotion. This suggested that the evolution of such advanced locomotor capabilities preceded the origin of crown-group amniotes. We here further investigate plausible body postures and locomotion of *Orobates* by taking soft tissues into account. Freely available animation software BLENDER is used to first reconstruct the lines of action of hindlimb adductors and retractors for *Orobates* and then estimate the muscle strain of these muscles. We experimentally varied different body heights in modeled hindlimb stride cycles of *Orobates* to find the posture that maximizes optimal strains over the course of a stride cycle. To validate our method, we used *Caiman crocodilus*. We replicated the identical workflow used for the analysis of *Orobates* and compared the locomotor posture predicted for *Caiman* based on muscle strain analysis with this species' actual postural data known from a previously published X-ray motion analysis. Since this validation experiment demonstrated a close match between the modeled posture that maximizes optimal adductor and retractor muscle strain and the *in vivo* posture employed by *Caiman*, using the same method for *Orobates* was justified. Generally, the use of muscle strain analysis for the reconstruction of posture in quadrupedal vertebrate fossils thus appears a promising approach. Nevertheless, results for *Orobates* remained inconclusive as several postures resulted in similar muscle strains and none of the postures could be entirely excluded. These results are not in conflict with the previously inferred moderately erect locomotor posture of *Orobates* and suggest considerable variability of posture during locomotion.

**Keywords: locomotion, posture, gait, extrinsic muscles, fossil, animation, muscle strain, virtual experiment**

## INTRODUCTION

The reconstruction of the biomechanics of fossils is a valuable approach to understand and investigate extinct life. While largely determining musculo-skeletal function, soft tissues like muscles are rarely preserved in fossils (Lautenschlager, 2016). However, with the development of new computational modeling techniques alternative possibilities to reconstruct and investigate the soft tissues of extinct species have emerged (Cunningham et al., 2014). In particular, the development and increasing availability of computed tomography (CT) had a fundamental impact on paleobiological research (e.g., Cunningham et al., 2014). Traditional reconstructions of soft tissues such as muscles were restricted to a theoretical, usually two-dimensional framework with drawings. The advent of CT not only allows the visualization of bone internal structures (Sutton, 2008; Cunningham et al., 2014), but also more sophisticated musculo-skeletal models (e.g., Bates and Falkingham, 2012; Hutchinson, 2012; Lautenschlager, 2015; Bishop et al., 2021). This potential to create three-dimensional models has led to a diversification of techniques to investigate fossils regarding functional morphology and biomechanical behavior including the role of soft tissues (Anderson et al., 2012; Cunningham et al., 2014; Manafzadeh and Padian, 2018; Demuth et al., 2020; Lautenschlager, 2020).

Modern Amniota represent a highly successful and diverse clade, comprising roughly 75% of extant tetrapods including lizards, snakes, turtles, crocodiles, birds, and mammals as well as a suite of large, but extinct radiations such as pterosaurs, sauropterygians, and non-avian dinosaurs (Reisz, 1997; Clack and Bénéteau, 2012). Fossil evidence suggests an origin of amniotes in the Carboniferous period (e.g., Laurin and Reisz, 1997; Clack, 2006; Coates and Ruta, 2007). Some authors argue that only with the evolution of the first amniotes, the transition of vertebrates to living on land was completed, because the reproduction was not directly dependent on open water anymore (Martin and Sumida, 1997; Nyakatura et al., 2014). This transition also necessitated the evolution of increasingly effective locomotion in terrestrial habitats.

To gain further insight into the locomotor characteristics of early amniotes, the focus of this study is on the extrinsic hindlimb muscles of the putative stem amniote *Orobates pabsti*. *Orobates* is a basal diadectid from the early to mid-Permian Tambach formation of central Germany (Berman et al., 2004). Diadectidae is most often hypothesized to represent the fossil sister group of Amniota (Laurin and Reisz, 1995, 1997; Lee and Spencer, 1997; Coates and Ruta, 2007), but *Orobates* also has been reconstructed within the crown group (Marjanović and Laurin, 2019). In addition to body fossils, fossil trackways were recovered from the same site, some of which could be assigned to *Orobates* as the trackmaker (Voigt et al., 2007). This combination of track and trackmaker offers a unique possibility to reconstruct the locomotion of this fossil species (Berman et al., 2004; Voigt et al., 2007; Nyakatura et al., 2015, 2019). A previous study integrated kinematic and dynamic modeling and employed a bioinspired robot to understand the locomotion of *Orobates* (Nyakatura et al., 2019). We here built on this previous study and utilized the modeling of soft tissues, specifically the muscle strain in the extrinsic hindlimb muscles, to further our understanding of the posture and locomotion in this key taxon. With this analysis of muscle strains we tested previous locomotor reconstructions in an independent way using a variant of multibody dynamics analysis (MDA). MDA is a computational analysis method including solid components connected by joints which restrict the movements by internal and external forces (Lautenschlager, 2020). It is a non-invasive method to simulate and test different scenarios and complex designs (Lautenschlager, 2015, 2020). The method was often used in comparative biomechanics research, e.g., to investigate human jaw movement (Koolstra and van Eijden, 1995), bite forces of theropod dinosaurs (Bates and Falkingham, 2012), or neck function in extinct vertebrates (Snively et al., 2013).

Here we simulated *Orobates* locomotion and used an MDA-like method linking rigid skeletal elements and simulating movements, but not accounting for forces. We modeled abstracted hindlimb adductor and retractors (reduced to a straight line of action) and quantified the occurring muscle strains of these muscles in diverse postures ranging from a "very low" (essentially belly-dragging) posture to a "very high" posture with maximally extended limbs at touch down. We aimed to identify the body posture which maximizes the occurrence of optimal muscle strains (and to identify anatomically implausible excessive compression/tension). Extrinsic hindlimb muscles are connecting the torso with the limb and are particularly important for posture and the generation of forward propulsion (Ashley-Ross, 1994; Fischer et al., 2002; Schilling et al., 2009). We, therefore, focused on extrinsic hindlimb muscles in this study. In terms of the posture of a sprawling tetrapod, the extrinsic hindlimb adductors depress the femur to pull the knee toward the sagittal plane and thus lift the trunk off the ground (Russell and Bels, 2001). In terms of the generation of propulsion, extrinsic hindlimb retractors pull the femur posteriorly and, when the foot is in contact with the ground, thereby propel the body forward.

The rationale of the modeling approach of this paper is based on the assumption that tetrapods engage postures and gaits during locomotion, which maximize the occurrence of optimal muscle strains. Importantly, we first tested this assumption in *Caiman crocodilus*, of which detailed 3D kinematics are known from a previous kinematic study using X-ray motion analysis (Nyakatura et al., 2019). It was tested whether a posture, as predicted by extrinsic hindlimb muscle strain analysis, matches the actual posture found in the kinematic analysis. Successful validation justified transferring our modeling approach to the extrinsic hindlimb muscles in *Orobates*. More generally, for the first time muscle strain analysis is used to constrain the reconstruction of the posture of a fossil tetrapod.

## MATERIALS AND METHODS

### Digital Model and Gait Simulation of *Caiman* Crocodilus

To first test the assumption of postures that minimize problematic muscle strains are being preferred, we validated the method using a modern amniote, *Caiman crocodilus*. An

available digital skeletal model of extant *Caiman crocodilus* from a previous study (Nyakatura et al., 2019) was used, an idealized gait was animated and different locomotor postures were simulated (Nyakatura and Demuth, 2019). *Caiman* kinematics are also known from a previous X-ray motion analysis (Nyakatura et al., 2019). If our assumption holds true, the methodology outlined above should be able to predict the naturally chosen posture of *Caiman*. Thus, we used the identical workflow that is used for the investigation of *Orobates* (detailed below) and compared the posture predicted for *Caiman* based on muscle strain analysis with this species' actual postural data known from X-ray motion analysis.

All procedures involving live animals were strictly following pertinent animal welfare regulations and were authorized by the Thüringer Landesamt für Verbraucher- und Umweltschutz (registration number: 02-008/11) in the state of Thuringia, Germany. Two *Caiman* individuals were originally borrowed from a zoo (La Ferme aux crocodiles, Pierrelatte, France) and analyzed (Nyakatura et al., 2019). After the investigation, the two borrowed *Caiman* were returned to the zoo unharmed. For this study, only videos of the female were selected for the idealized animation of the complete skeletal movement during locomotion, to directly match its skeleton to its movement.

We created an idealized animation based on a collage of X-ray videos to capture the movement of the whole skeleton (**Supplementary Video 1**). When passing by the 38 cm image intensifiers of the system, only a part of the individual was within the field of view. A set of a synchronized dorsal and a lateral video of the *Caiman* walking through this narrow field of view was imported into ADOBE AFTER EFFECTS (Adobe Inc., San José, California, United States). The videos were duplicated several times and they were arranged and timed in such a way that the impression of an X-ray video with a much-extended field of view showing almost the entire specimen emerged (see **Supplementary Video 1**). This visualization was first conceived and prepared by Jonas Lauströer (as part of our previous study Nyakatura et al., 2019), but was later on improved by one of us (OED). This allowed us to montage an X-Ray video of the entire skeleton for a complete, idealized walk cycle of *C. crocodilus*.

The 3D bone models were obtained from medical CT data collected at the Friedrich Schiller University Hospital and segmented in the software package AMIRA (Thermo Fisher Scientific, Zuse Institut Berlin, Germany) (Nyakatura et al., 2019). Using these 3D bone models, a digital marionette of the female *C. crocodilus* (specimen no.: PMJ Rept 665, Phyletisches Museum Jena, Germany) was created, scaled to match the video, and superimposed onto the idealized X-ray collage (**Figure 1**). A hierarchical joint marionette (Gatesy et al., 2010; Arnold et al., 2014), i.e., an inverse kinematic (IK) rig (Watt and Watt, 1992), was used to match the bones with their x-ray shadows in the software package AUTODESK MAYA (Version 2015; Autodesk Inc., San Rafael, California, United States) (see Wiseman et al., 2021). For further analysis, the model was transferred from AUTODESK MAYA into BLENDER.

Actual kinematic data of *Caiman crocodilus* was measured *in vivo* using XROMM (X-ray reconstruction of moving morphology; Brainerd et al., 2010) in a previous study (Nyakatura et al., 2019 cf. SM14 of the cited reference). These published data were then used to evaluate the model predicted posture, which maximizes optimal muscle strains, against *in vivo* kinematic data.

## Digital Model and Gait Simulation of *Orobates pabsti*

The digital version of the holotype specimen of *Orobates pabsti* (specimen number MNG 10,181) was available for this study (Nyakatura et al., 2015, 2019). Moreover, we used the animated digital skeleton from a previous study (Nyakatura et al., 2019). Please refer to our previous publications for specifics of how the digital specimen was generated and the rationale for animation properties (Nyakatura et al., 2015, 2019; Nyakatura, 2017, 2019). In brief, the holotype specimen was microCT-scanned and individual bone fragments were segmented and thus freed from the surrounding rock matrix. Bone fragments of a single skeletal

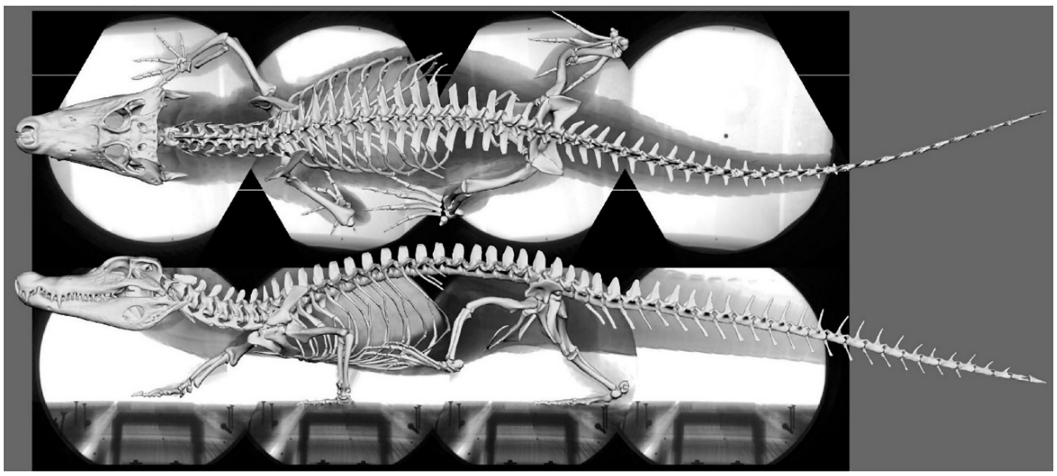

**FIGURE 1 |** Superimposed skeleton on the X-ray video collage in dorsal (top) and lateral (bottom) view (**Supplementary Video 1**).

element were fused and all skeletal elements were undistorted (Nyakatura et al., 2015). For the animated step cycle, fossil trackways assigned to *Orobates* (cf. Voigt et al., 2007) were analyzed and used as a hard constraint, i.e., each manus and pes was forced to match the trackways (Nyakatura, 2019; Nyakatura et al., 2019). Limb and spine kinematics were animated in accordance with general biomechanical principles of sprawling tetrapod locomotion identified in a previous study and were anatomically plausible in terms of joint mobility (Nyakatura et al., 2019). Specifically, this refers to the relationship of stylopodial long-axis rotation to stylopodial protraction/retraction.

Importantly, the Maya rig controlling *Orobates*' simulated locomotion as well as the rig controlling *Caiman* allowed to set and adjust body height (i.e., lifting of the trunk off the ground; cf. Nyakatura et al., 2019). Despite using the same set of hip kinematics for all of our modeled body heights, this affected not only femoral adduction/abduction, but also resulted in changes of protraction/retraction and long-axis rotation due to the interdependency of rotations when describing 3D joint movements with Euler angles (Sullivan, 2007). Like the model of *Caiman,* the model of *Orobates* was transferred into BLENDER as .fbx files which retained the movement and animation paths of the rigs. To simplify the model only the movement sequence of the hindlimb was used. The rest of the skeletal elements were combined in a single component as the movement of these was not necessary for the study.

## Abstracted Muscle Models and Analysis of Muscle Strains

Muscles fibers are made up of myofibrils which consist of contractile units, the sarcomeres. Within the sarcomeres, crossbridges between overlapping Myosin and Actin filaments are built. Contraction is realized through a conformation change of Myosin heads and resulting relative movement between the linked filaments (i.e., the power stroke). Due to this internal structure, muscles have a tension/compression range in which a maximum tetanic contraction can be achieved (Sherwood et al., 2013). The optimal range for the generation of force is between 70 and 130% of resting length, while maximum compression and tension of a muscle is approximately reached at 30 and 170% of resting length, respectively (Sherwood et al., 2013; Lautenschlager, 2015). Thus, simulated step cycles that invoke muscle compression below 30% and tension beyond 170% resting length can be regarded as problematic and are considered here as unlikely to occur in cyclic, steady-state walking. More generally, we expect animals to choose gaits and postures that maximize optimal muscle strains (and minimize problematic muscle compression and extension).

For the modeling of abstracted muscles and for the analysis of muscle strains of *Caiman* and *Orobates* the freely available three-dimensional (3D) visualization software BLENDER[1] was used, which allows the animation and manipulation of models (Garwood and Dunlop, 2014). This software also provides the possibility for analytical approaches and automatization using the in-built python interpreter (Lautenschlager, 2015). For measuring the muscle strain over the course of a step cycle, a python script was created which measures the strain of each muscle and calculates the muscle strain ratios between a defined reference length (see below) and stretched/compressed muscle conditions. Data of all recorded parameters were automatically exported to a text file for post-processing.

In the digital models of *Caiman* and *Orobates*, the hindlimb could be moved relative to the pelvis. First, the muscles of the adductors and retractors were reconstructed in each model. The following primary hindlimb adductors critical for the animals' hip height were considered in this study: *M. adductor femoris* (ADD), *M. puboischiofemorales externus* (PIFE), *M. puboischiotibialis* (PIT). In addition to the adductors, we also modeled the primary retractors of the femur and thus hindlimb of sprawling tetrapods: *M. caudofemoralis longis* (CFL) and *M. caudofemoralis brevis* (CFB).

For *Caiman* the muscle origins and insertions were modeled in accordance with a detailed anatomical description of *Caiman latirostris* (**Figure 2**; Otero et al., 2010). Muscle reconstruction in fossils is challenging, as they are often not preserved. Yet, reconstruction of *Orobates*' muscles was critical for the purpose of this study. One widely used approach to infer the presence of soft-tissues in fossil vertebrates is the examination of the extant phylogenetic bracket (Witmer, 1995). This involves comparing the osteological attachments sites in fossil species with extant taxa (Molnar et al., 2020; Bishop et al., 2021). The muscle attachment sites in *Orobates* were determined by comparing the presence of muscles in modern amphibians and modern selected sprawling amniotes using published anatomical descriptions (we did not consider highly derived amniote postcrania represented in e.g., mammals, turtles, snakes, or birds). For this purpose, various previous studies that reported muscle attachment sites (Ashley-Ross, 1992; Otero et al., 2010; Diogo et al., 2016; Molnar et al., 2020) were examined for differences and similarities in extrinsic hindlimb muscles between amphibians and sprawling amniotes. Based on this, we inferred the presence or absence of these muscles as well as their attachment sites for *Orobates* (see "Results"). Importantly, the 3D reconstructed bone models of *Orobates* (from Nyakatura et al., 2015) lack obvious morphological indicators of muscle attachments and the reconstruction of simplified muscle lines of action, therefore, remains uncertain.

In BLENDER the muscles were abstracted as simple cylinders between the origin and the insertion, thus along a straight line of action (Lautenschlager, 2015). The ends of each cylinder representing a muscle were fixed to the reconstructed muscle attachment sites on the bone models. Although these muscle models can potentially penetrate bones and one another, it was not observed in any of our modeled trials. Thus, when joint movement was animated and the skeletal elements were moved relative to one another, the cylinders were compressed or stretched. We defined the reference length (i.e., 100% muscle length in our models) to occur at 50% of the contact phase, i.e., at mid-stance. Here the assumption is made that at mid-stance limb

[1] www.blender.org; version 2.81

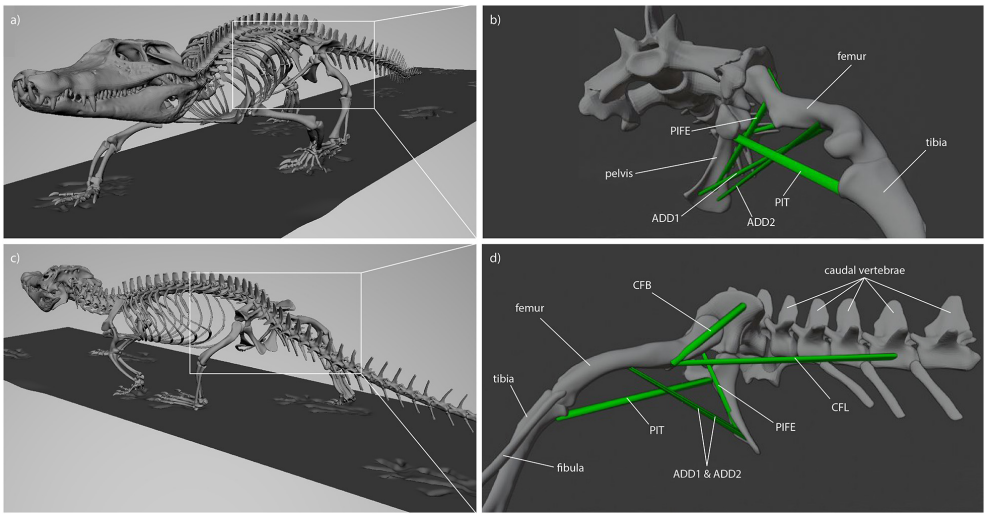


**FIGURE 2 |** Muscle attachments and lines of action in *Caiman* (see Otero et al., 2010). **(a)** Latero-frontal view of *Caiman*, **(b)** latero-frontal view of relevant skeletal elements to show adductor muscles (ADD1, ADD2, PIFE 3rd head, PIT) at reference length (mid-stance), **(c)** latero-caudal view of *Caiman*, **(d)** latero-caudal view of relevant skeletal elements to show retractor muscles (CFB, CFL) at reference length (mid-stance).

posture resembles posture of still-standing animals and presents a replicable posture. For each modeled body height (see below) all muscle strain measures were taken relative to the mid-stance reference pose.

## Modeling Postures

To be able to identify postures in which problematic muscle strains were minimized, we modeled multiple different postures in our simulated stride cycles in a "virtual experiment" (Nyakatura and Demuth, 2019). Particularly, we analyzed muscle strains in five simulated postures characterized by different degrees of sprawling (**Figure 3**): "very low," "low," "intermediate," "high," and "very high." We consider the "very low" and the "very high" postures to encompass anatomical plausibility. In the "very low" posture the limb posture at various instances during the stride cycle was "hypersprawled," i.e., the knee is positioned more dorsal than the hip and the belly is in contact with the ground (Nyakatura et al., 2014). In the "very high" posture the hindlimb was extended as much as possible at touch down and any further extension would have resulted in disarticulated joints (see Nyakatura et al., 2019). "Low," "intermediate," and "high" postures were modeled at evenly spaced increments between these extremes. Additionally, the modeled postures were also quantified using hip height expressed as percentage of inter girdle distance (IGD) at mid-stance in order to provide a way to replicate the modeled postures. Note that the different modeled postures did not occur at identical relative hip heights. In *Caiman* these vary from IGD 0.28 ("very low" posture) to 0.69 ("very high" posture) (**Figure 4**). In *Orobates*, these vary from the IGD 0.37 ("very low" posture) to 0.52 ("very high" posture) (**Figure 5**).

In order to identify the posture for *Orobates* which minimizes excessive strains, we used the identical workflow that was used for *Caiman*. Therefore, for each modeled muscle of both models (*Caiman*, *Orobates*) and for all five simulated postures, the muscle strain was measured over the course of the simulated stride cycle. The estimated muscle strains were plotted against the percentage of the stride cycle. To visualize whether muscle strains during a stride cycle at a specific simulated posture are involving problematic values, we highlighted the respective areas in the graphs. In these graphs, the green area represents optimal compression/tension muscle strains (i.e., within 70 and 130% of reference length), the orange area represents non-optimal, but feasible strains, and the red area indicates that compression/tension are no longer considered possible (i.e., below 30% and above 170%). For each modeled hip height, we then determined the percentage of the stride in which optimal strains were maintained and used this percentage as a metric for comparison between simulated postures following the principle "the-higher-the-value-the-better," but body heights that induced muscle strains $<30$ and $>170\%$ were ruled out.

# RESULTS

## Validation: *Caiman* Crocodilus

Taking all simulated postures together, in *Caiman* muscle strain values for ADD1 ranged from 93 to 203% and for ADD2 from 94 to 190% over the course of a stride cycle (**Figures 6A,B**). These two muscles showed the greatest range of values. For the muscles PIFE3 and PIT, we measured values of 99–115% and 95–127%, respectively (**Figures 6C,D**). The femoral retractors CFB and CFL exhibited values from 44 to 114% and 76 to 111%, respectively, over the course of a step cycle (**Figures 6E,F**).

In the "very high" posture (IGD = 0.69) the highest strains for the adductor's ADD1 and ADD2 occurred. These were $>170\%$

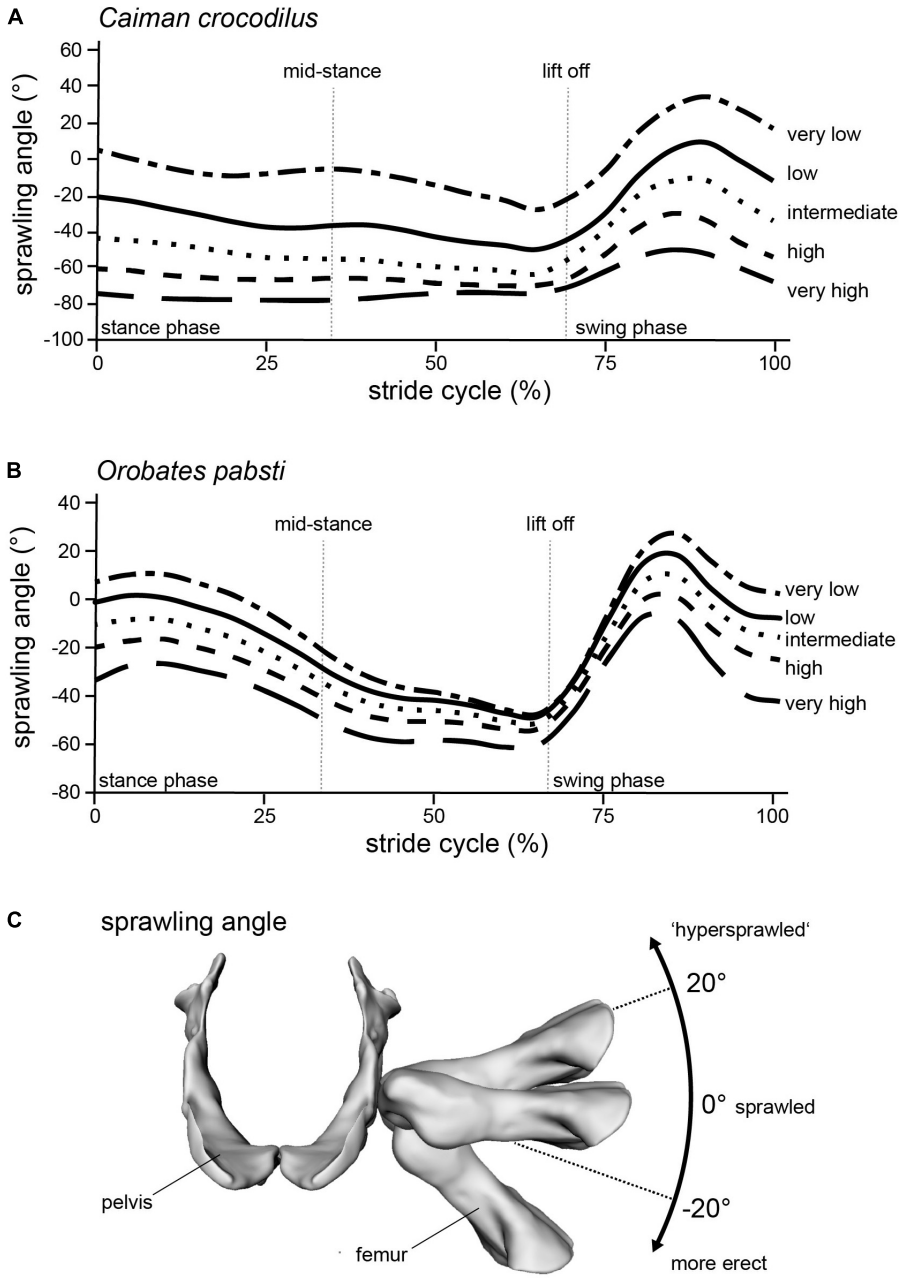


**FIGURE 3 |** Modeling different postures from "very low" to "very high" in **(A)** *Caiman* and **(B)** *Orobates* is reflected in the **(C)** sprawling angle (frontal view of the pelvis and femur of *Orobates* with differently ad/abducted femur). Raw data provided as **Supplementary Material**.

of reference length (**Figures 6A,B**). Also, the CFB showed strains out of the optimal tension area (**Figure 6E**).

Skeletal muscle here is only considered to function properly at a strain value of > 30 and < 170% of the reference length. Only the "very high" posture involved implausible strains and was excluded as a possibility for *Caiman*. In turn, all other simulated body heights were considered plausible reflecting the diverse locomotor postures observed in modern crocodilians from "low walks" to "high walks." However, at the "low" and "intermediate" postures (IGD of 0.39 and 0.49) not only entirely avoided implausible muscle strains, but also strains remained within the optimal length (i.e., > 70 and < 130% of reference length; the green areas in **Figures 4**, **6**) for an average of above 95% for all six modeled muscles over the course of the stride cycle (**Table 1**). Our modeling approach thus predicts that *Caiman* adopts a "low" to "intermediate" hip height in accordance with the assumption that optimal muscle strains are maximized and critical muscle strains are avoided in living animals. Indeed, the value for the "intermediate" posture model almost exactly matched *in vivo Caiman* data which documented hip height of

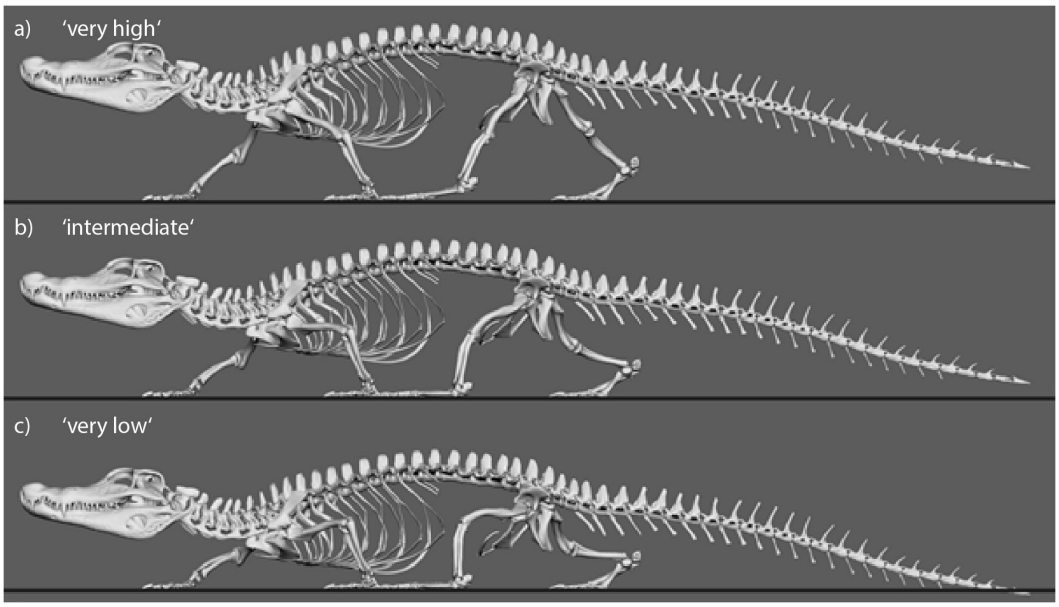


**FIGURE 4 |** Still images from animated *Caiman* locomotor cycle to illustrate the experimental variation of body height. Three of five variations are shown. **(a)** "Very high" with IGD = 0.69. **(b)** "Intermediate" with IGD = 0.49. **(c)** "Very low" with IGD = 0.29.

IGD = 0.502 (± 0.021) (Nyakatura et al., 2019; the specimens of *Caiman* never chose low walks in this previous study). We used this close match as a justification to employ our muscle strain modeling approach to the simulated gaits of *Orobates pabsti*.

## Muscle Attachments in *Orobates* Hindlimb and Proposed Function

Reconstruction of muscle line of actions is a necessary prerequisite for the modeling of muscle strains in *Orobates*. Several adductors contribute to hip height and thus posture. During the contact phase, ADD1 prevents the limb from collapsing by resisting femoral abduction. The muscles ADD2, *M. puboischiotibialis* (PIT) and PIFE assist in this function (Gatesy, 1997; Hutchinson and Gatesy, 2000). In *Caiman* the *M. adductor femoris* (ADD) is comprised of two heads, the *M. adductor femoris 1* (ADD1) and *M. adductor femoris 2* (ADD2), with longitudinal fibers and triangular shape (Otero et al., 2010; **Figure 2**). ADD1 originates over the anterolateral surface of the ischium, close to the obturator process and inserts along the posterior surface of the femoral shaft. ADD2 has its origin on the postero-lateral portion of the ischium and also inserts along the posterior surface of the femoral shaft *in Caiman*. The muscles ADD1 and ADD2 are separated through *M. puboischiofemoralis externus* (PIFE) (Otero et al., 2010). In salamanders, the *adductor femoris* muscle is also present but has only one head that features the same origin and insertion sites of ADD1 in *Caiman* (Diogo et al., 2016; Molnar et al., 2020). In diadectids (which include *Orobates*) the muscle attachment sites are wider (Romer, 1922) suggesting a similar triangular shape as in *Caiman*. Therefore in *Orobates* two muscle portions were modeled and examined for the adductors (ADD1, ADD2; **Figure 7**). The PIT is a small muscle that arises in *Caiman* from the anterolateral surface of the ischium and inserts on the proximomedial aspect of the tibia (Otero et al., 2010). In salamanders this muscle originates from the puboischiac plate and inserts on the proximal two-thirds of the anteromedial face of the tibia (Ashley-Ross, 1992). Because of the similarities in origin and insertion of the PIT in both the amniote *Caiman* and anamniote salamanders, we reconstruct similar muscle attachment points in *Orobates*. The PIFE is undivided in non-archosaurian taxa (Hutchinson, 2001). This muscle also assists in the adduction of the femur and therefore prevents the body from collapsing to the ground. In *Caiman* the PIFE has three heads, in our study we investigate the third head of PIFE (i.e., PIFE3) which originates on the lateral aspect of the ischium between ADD1 and ADD2 and inserts on the major trochanter of the femur (Gatesy, 1997; Hutchinson and Gatesy, 2000; Otero et al., 2010). In amphibians like salamanders an undivided PIFE arises from the lateral aspect of the ischium and inserts onto the femoral trochanter (Ashley-Ross, 1992). In *Orobates* we modeled an undivided muscle. However, the muscle attachment sites in Archosauria for PIFE3 and PIFE in amphibians are similar, thus we assumed the same muscle attachment (**Figure 7**).

*M. caudofemoralis longis* (CFL) and *M. caudofemoralis brevis* (CFB) are the main retractors of the femur. In archosaurs like *Caiman* the CFL has its origin from the lateral sides of haemal arches and the base of proximal caudal vertebral centra. This muscle joins the CFB to insert via a tendon on the fourth trochanter of the femur (Otero et al., 2010). The smaller muscle CFB lays anterior to the CFL and has two sites of origin in *Caiman*. The first arises from the postero-ventral part of the illium and the second site arises from the centrum and the base of the transverse processes of the anterior caudal vertebrae.

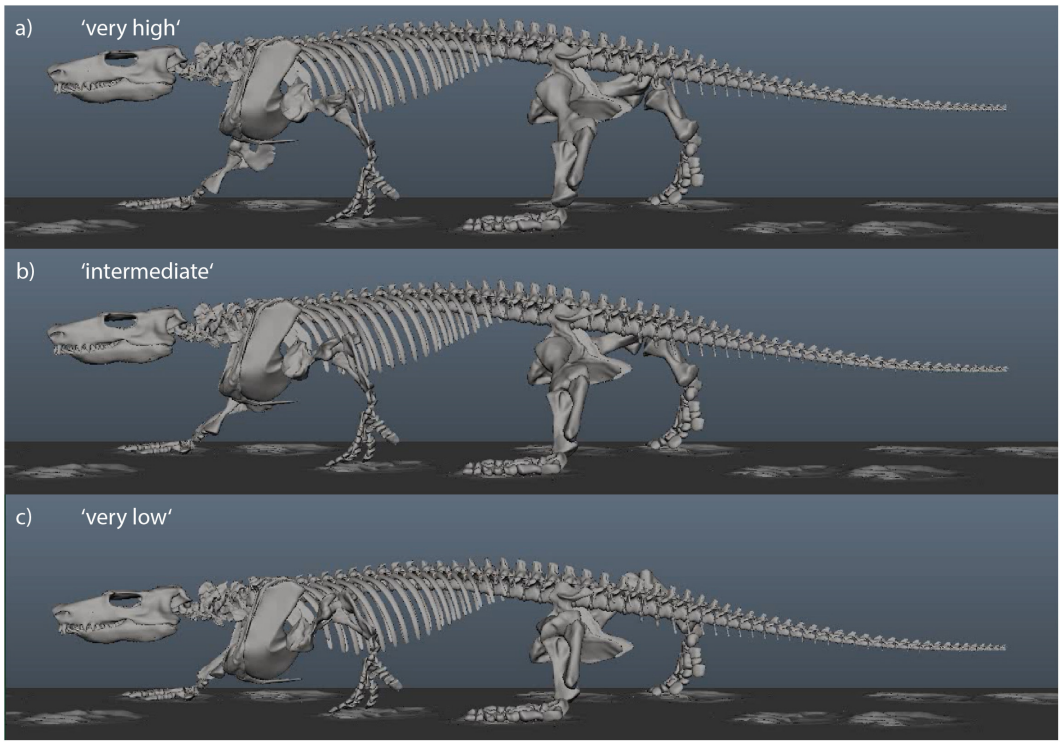


**FIGURE 5 |** Still images from animated *Orobates* locomotor cycle to illustrate the experimental variation of body height. Three of five variations are shown. Animation from Nyakatura et al. (2019). **(a)** "Very high" with IGD = 0.52. **(b)** "Intermediate" with IGD = 0.45. **(c)** "Very low" with IGD = 0.38.

The muscle inserts on the femur close to the fourth trochanter (Gatesy, 1997; Otero et al., 2010). In salamanders just one portion of the *M. caudofemoralis* is usually distinguished and shares the same muscle attachment sites like the CFL in archosaurs (Ashley-Ross, 1992; Molnar et al., 2020). As with the ADD, the muscle attachment site of the *M. caudofemoralis* is wider in Diadectidae (Romer, 1922). Therefore, we again used two muscle portions to examine the muscle strain of the *caudofemoralis* in *Orobates* (we distinguished between CFL and CFB in *Orobates*; **Figure 7**).

Obvious sites of attachment for any of these muscles were not visible on the 3D reconstructed bone models of *Orobates pabsti* (from Nyakatura et al., 2015) and reconstructed muscle attachment sites should therefore be treated with caution.

## Muscle Strain Analysis for *Orobates* Pabsti

Taking all simulated postures together in *Orobates* muscle strain values for ADD1 ranged from 82 to 108% and for ADD2 from 68 to 123% over the course of a stride cycle (**Figures 8A,B**). For the muscles PIFE and PIT we measured values of 44–156% and 93–133%, respectively (**Figures 8C,D**). The femoral retractors CFB and CFL displayed values ranging from 39 to 150% and from 61 to 123% over the course of a stride cycle (**Figures 8E,F**). None of the simulated postures involved strain values of $< 30$ or $> 170\%$ of reference length. Thus, all simulated postures (from "very low" to "very high") can be considered plausible and no posture can be discarded outright. The absolutely highest strain values were found at the "very high" posture with peak PIFE muscle strain of 156.33% of reference length. The absolutely lowest muscle strain value occurred in the CFB at the "high" posture (with a minimum value of 39.65% of reference length). The least critical body posture for *Orobates* was found to be "intermediate" (89.24% optimal strain values across all muscles over the entire stride cycle), but the "very low" (88.59%) and the "high" (88.98%) postures similarly maximized the occurrence of optimal muscle strains between 70 and 130% of the reference length (**Table 2**).

# DISCUSSION

The aim of this study was to predict plausible body height (posture) and therefore further constrain the locomotion of the stem amniote *Orobates pabsti* by taking soft tissues, specifically the extrinsic hindlimb muscles, into account. In our modeling approach, we estimated the muscle strains of six muscles in five simulated body postures from "very low" to "very high." We identified postures for *Orobates* that maximize optimal strains over the course of a stride cycle. The identical workflow was first used for *Caiman crocodilus* to validate our modeling approach since for *Caiman* the model-predicted values could be compared to *in vivo* postural data from a previous study (Nyakatura et al., 2019). Although only the "very high" posture could be eliminated outright due to the occurrence of implausible strains, we found a

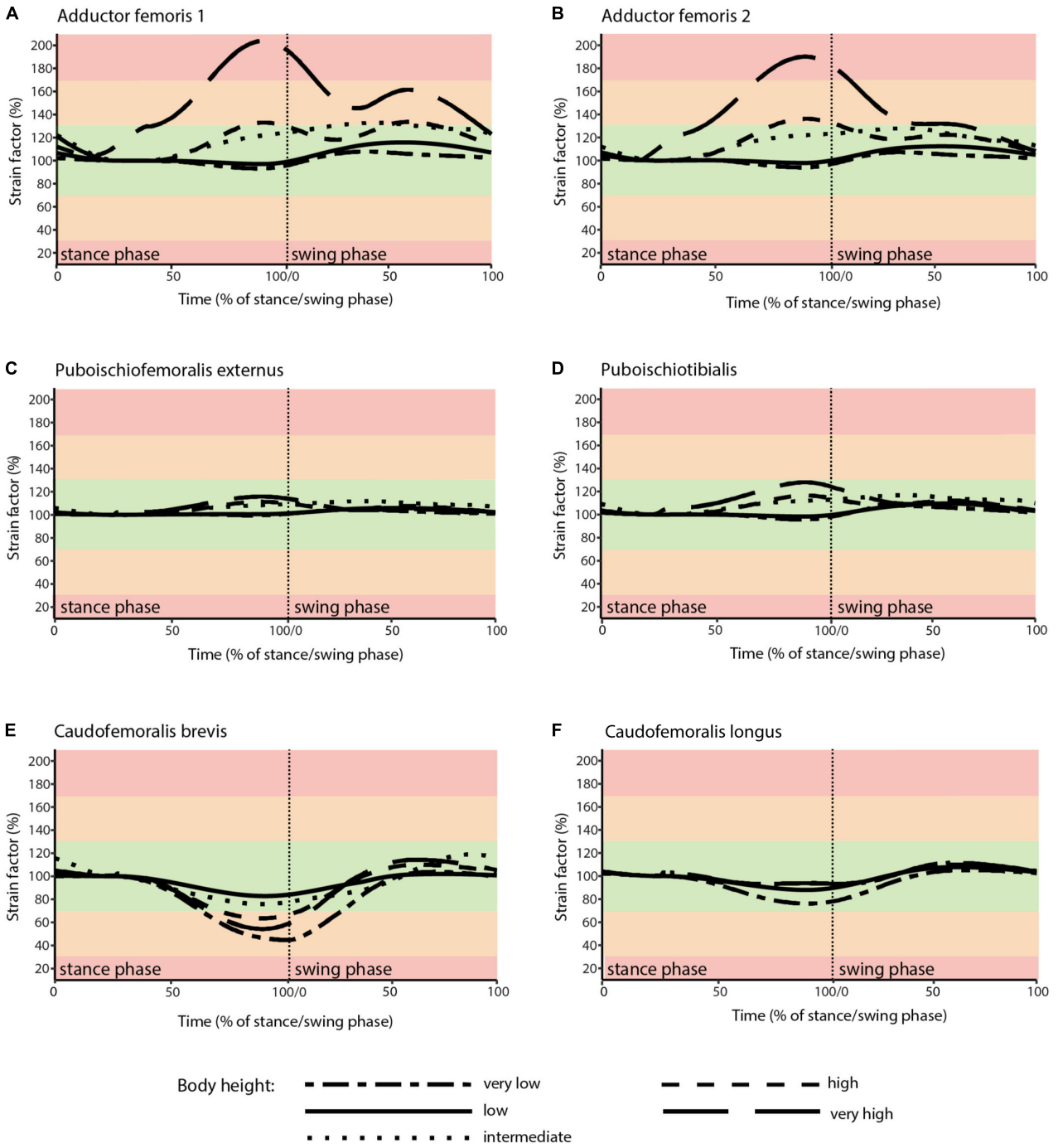


**FIGURE 6 |** Muscle strains plotted against percentage of stance and swing phase in *Caiman* for each of the five analyzed body heights. **(A)** ADD1; **(B)** ADD2; **(C)** PIFE; **(D)** PIT; **(E)** CFB; **(F)** CFL. Red areas of the plots involve muscle tension beyond 170% or compression below 30% of reference length and were considered implausible in this study. Green areas of the plots represented optimal muscle length for the generation of force (between 70 and 130% of reference length). Orange areas represent feasible muscle strains with limited potential for force generation.

close match between the predicted posture (maximizing optimal strains) and the *in vivo* posture of *Caiman* and used this to justify employing our modeling approach to *Orobates*.

Previous work into the reconstruction of *Orobates*' locomotor capabilities relied on information provided by fossil trackways (Voigt et al., 2007) and integrated kinematic and dynamic simulations as well as biorobotics (Nyakatura et al., 2019). This previous work proposed a relatively erect (intermediate to high body height with no belly dragging) posture, which was further interpreted to indicate a balanced and mechanical energy-saving

**TABLE 1 |** Percentage of the stride cycle that each modeled muscle maintained optimal muscle strain (i.e., within 70 and 130% of reference length) in *Caiman*.

| | Hip height | PIT | PIFE3 | ADD1 | ADD2 | CFB | CFL | Total |
|---|---|---|---|---|---|---|---|---|
| Stance phase | "Very low" | 100% | 100% | 100% | 100% | 62.5% | 100% | |
| | "Low" | 100% | 100% | 100% | 100% | 100% | 100% | |
| | "Intermediate" | 100% | 100% | 100% | 100% | 100% | 100% | |
| | "High" | 100% | 100% | 82.5% | 73.75% | 70% | 100% | |
| | "Very high" | 100% | 100% | 41.25% | 43.75% | 65% | 100% | |
| Swing phase | "Very low" | 100% | 100% | 100% | 100% | 75.71% | 100% | |
| | "Low" | 100% | 100% | 100% | 100% | 100% | 100% | |
| | "Intermediate" | 100% | 100% | 58.75% | 100% | 100% | 100% | |
| | "High" | 100% | 100% | 74.29% | 95.71% | 95.71% | 100% | |
| | "Very high" | 100% | 100% | 5.71% | 35.71% | 90% | 100% | |
| Complete stride cycle | "Very low" | 100% | 100% | 100% | 100% | 69.11% | 100% | 94.85% |
| | "Low" | 100% | 100% | 100% | 100% | 100% | 100% | 100% |
| | "Intermediate" | 100% | 100% | 79.38% | 100% | 100% | 100% | 96.56% |
| | "High" | 100% | 100% | 78.4% | 84.73% | 82.86% | 100% | 90.99% |
| | "Very high" | 100% | 100% | 23.48 | 39.73% | 77.5% | 100% | 73.45% |

*ADD, M. adductor femoris; PIFE, M. puboischiofemorales externus; PIT, M. puboischiotibialis; CFL, M. caudofemoralis longis; CFB, M. caudofemoralis brevis. See **Figure 6** for graphical illustration of muscle strains.*

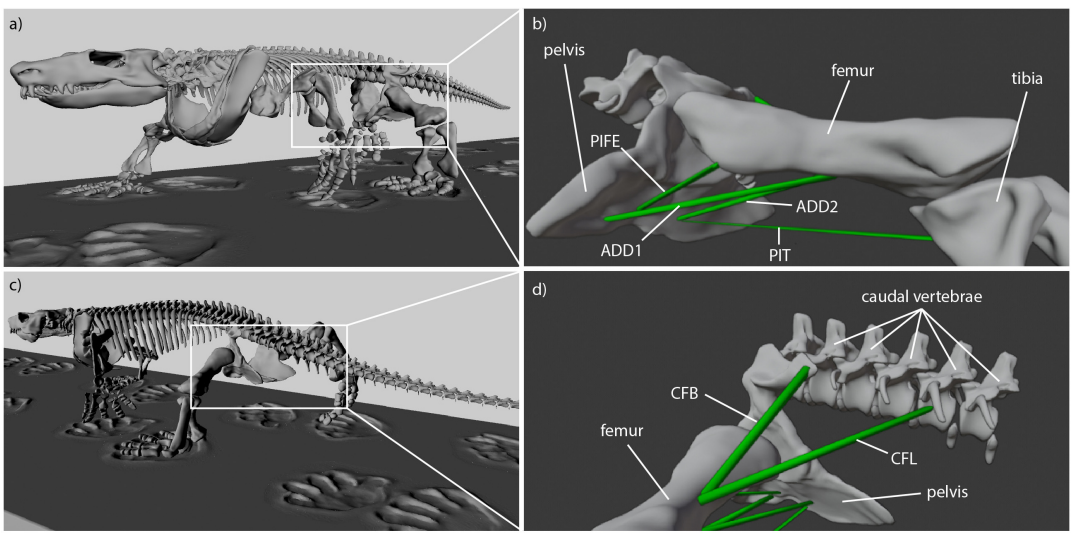


**FIGURE 7 |** Reconstructed muscle attachments and lines of action in *Orobates*. **(a)** Latero-frontal view of *Orobates*, **(b)** latero-frontal view of relevant skeletal elements to show adductor muscles (ADD1, ADD2, PIFE, PIT) at reference length (mid-stance), **(c)** latero-caudal view of *Orobates*, **(d)** latero-caudal view of relevant skeletal elements to show retractor muscles (CFB, CFL) at resting length (mid-stance).

gait (Nyakatura et al., 2019). Especially the latter previous quantitative study lends support to earlier qualitative assessments of *Orobates*' locomotion which hypothesized this species to have been capable of "increased speed, greater maneuverability, and more efficient support" than earlier tetrapods (Berman and Henrici, 2003). While uncertainty was acknowledged and even a website was published alongside the paper to allow readers to explore the gaits of *Orobates* and the consequences of changes made to any of the tested kinematic variables[2], several of the most plausible gait solutions identified for *Orobates* –including the solution featured in the main text of the paper– clustered around a body height of 44% IGD. Our results based on the assessment of muscle strains in various simulated gaits with differing body heights found the strongest support for an "intermediate" body height (45% IGD; but note that other modeled body heights yielded almost equal results within a single percentage point). Thus, the results of the current study based on an independent line of evidence do not directly contradict and one of the favored models is in agreement with a moderately erect posture and gait of *Orobates* (but see discussion of limitations to the here used approach below).

The presence of such more erect limb posture when compared to earlier tetrapods (Kawano and Blob, 2013; Nyakatura et al., 2014) suggests the capability to facilitate improved acceleration

[2]https://go.epfl.ch/Orobates

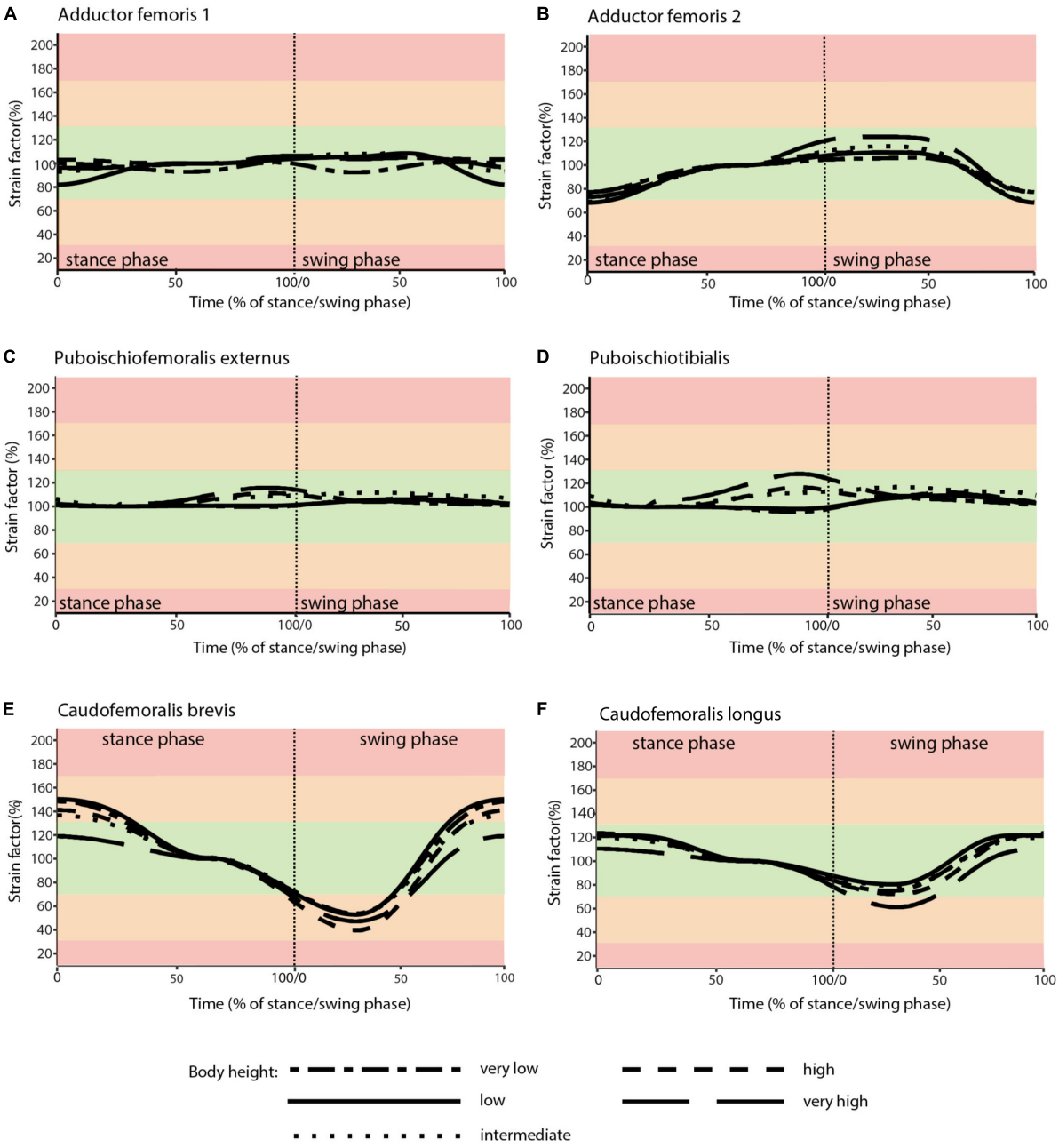


**FIGURE 8 |** Muscle strains plotted against percentage of stance and swing phase in *Orobates* for each of the five analyzed body heights. **(A)** ADD1; **(B)** ADD2; **(C)** PIFE; **(D)** PIT; **(E)** CFB; **(F)** CFL. Red areas of the plots involve muscle tension beyond 170% or compression below 30% of resting length and is considered implausible in this study. Green areas of the plots represented optimal muscle length for the generation of force (between 70 and 130% of reference length). Orange areas represent feasible muscle strains with limited potential for force generation.

of the body into the direction of travel (Riskin et al., 2016), greater overall capacity for speed (Reilly et al., 2005; Fuller et al., 2011), and reduced torsional stresses at limb long bone midshafts (Blob, 2001). Our results thus lend further tentative support to the possibility of such advanced locomotion (as outlined in the previous sentence) already present in the last common ancestor of diadectids and crown amniotes. Given the most common recovered phylogenetic position of diadectids as stem amniotes (e.g., Laurin and Reisz, 1995, 1997; Lee and Spencer, 1997; Coates and Ruta, 2007), this would imply that advanced terrestrial locomotion beneficial to navigating fully terrestrial habitats preceded the origin of crown amniotes in contrast to previous suggestions (Sumida and Modesto, 2001).

While the earlier study of Nyakatura et al. (2019) used complex permutations of several interdependent variables of sprawling tetrapod locomotion, the current study focuses solely

**TABLE 2 |** Percentage of the stride cycle that a modeled muscle maintained optimal muscle strain (i.e., within 70 and 130% of reference length) in *Orobates*.

| | Hip height | PIT | PIFE | ADD1 | ADD2 | CFB | CFL | Total |
|---|---|---|---|---|---|---|---|---|
| Stance phase | "Very low" | 100% | 78.75% | 100% | 100% | 70.00% | 100% | |
| | "Low" | 100% | 71.25% | 100% | 91.25% | 67.50% | 100% | |
| | "Intermediate" | 100% | 81.25% | 100% | 93.75% | 78.75% | 100% | |
| | "High" | 87.50% | 100% | 100% | 100% | 68.75% | 100% | |
| | "Very high" | 100% | 91.25% | 100% | 100% | 97.50% | 100% | |
| Swing phase | "Very low" | 100% | 84.29% | 100% | 100% | 30.00% | 100% | |
| | "Low" | 74.29% | 74.29% | 100% | 92.86% | 27.14% | 100% | |
| | "Intermediate" | 100% | 85.71% | 100% | 94.28% | 37.14% | 100% | |
| | "High" | 92.86% | 91.43% | 100% | 100% | 27.14% | 100% | |
| | "Very high" | 100% | 34.29% | 100% | 100% | 45.71% | 61.43% | |
| Complete stride cycle | "Very low" | 100% | 81.52% | 100% | 100% | 50% | 100% | 88.59% |
| | "Low" | 87.15% | 72.77% | 100% | 92.06% | 47.32% | 100% | 83.22% |
| | "Intermediate" | 100% | 83.48% | 100% | 94.02% | 57.95% | 100% | 89.24% |
| | "High" | 90.18% | 95.72% | 100% | 100% | 47.95% | 100% | 88.98% |
| | "Very high" | 100% | 62.77% | 100% | 100% | 71.61% | 80.72% | 85.85% |

*ADD, M. adductor femoris; PIFE, M. puboischiofemorales externus; PIT, M. puboischiotibialis; CFL, M. caudofemoralis longis; CFB, M. caudofemoralis brevis. See **Figure 8** for graphical illustration of muscle strains.*

on one kinematic variable, which is body height (as reflected by the sprawling angle or expressed as percentage of IGD). The influence of body height was tested, but other hip kinematic properties (pro-/retraction, long-axis rotation) were unavoidably affected by the IK rig due to the interdependency of rotations when using Euler angles to describe 3D joint movements (Sullivan, 2007). In addition to this, it remains unexplored what consequences systematic changes to other kinematic variables of sprawling locomotion such as long-axis rotation, pre-/retraction, and spine bending (Barclay, 1946; Ashley-Ross, 1994; Karakasiliotis et al., 2016) have on the muscle strains of the extrinsic hindlimb muscles in *Orobates*. Moreover, we cannot fully exclude any of the tested body heights for *Orobates*, because none of them reached implausible values of muscle tension (>170% of resting length) or muscle compression (<30% of resting length) (Sherwood et al., 2013; Lautenschlager, 2015). Hence, even though the "intermediate" posture reached the overall maximized optimal muscle strains, data for muscle strain assessed here remains inconclusive, but does not contradict previous reconstructions of posture and gait for *Orobates*. Animals generally engage in diverse behaviors that often involve larger joint excursions and thus also muscle strains than cyclic steady-state walking. *Orobates* was potentially capable of locomotion at different body heights (cf. the "low walks" and "high walks" of crocodiles, e.g., Gatesy, 1991; Reilly et al., 2005). Regardless, the results derived from our modeling approach should be considered tentative steps into the incorporation of soft tissue anatomy into the reconstruction of locomotor properties.

We acknowledge that the muscle models used here are highly abstracted and simplified. It is, however, very encouraging that this simple approach was capable of closely predicting the *in vivo* posture exhibited in our validation experiments using the *Caiman*. Again, "low" and "intermediate" (hip height of 0.49 IGD) postures maximized optimal muscle strains over the course of an entire stride, almost matching the *in vivo* hip height of 0.5 IGD *in vivo*. The degree of muscle tension and compression is most relevant during activity of a muscle (although even during inactivity the risk of muscle injury remains). Available electromyographic (EMG) data for *Caiman* is scarce, but Gatesy (1989) mentioned that the observed preliminary data of the extrinsic hindlimb muscles of *Caiman crocodilus* (referred to by its synonym *Caiman sclerops* in Gatesy, 1989) appear to be similar to more robust data from *Alligator mississippiensis*. While in our analysis the most critical muscle strains occur in the ADD1 and ADD2 as well as in the CFB muscles during late stance and swing phase, available EMG data points to reduced activity of postural and propulsive muscles of crocodilians during that time of the stride cycle. Importantly, however, to our knowledge no data has been published for the ADD2 and CFB muscles in either *Alligator* or in *Caiman* highlighting the need for such *in vivo* muscle activation pattern data. Still, our validation was able to predict the posture of *Caiman*, albeit that other postures scored similarly high. This validation lends support, not only for the transfer of our method to the modeling of *Orobates*' locomotion, but also to the more general assumption we made here. Specifically, we hypothesized that tetrapods will choose postures and gaits that will maximize the occurrence of optimal muscle strains. While this clearly needs further empiric evidence from other species, when further corroborated this relationship could be utilized for the inference of posture and gaits in other fossil taxa, too.

Further simplifications in the model setup were made, such as modeling muscles as simple point-to-point connections. In reality, however, muscles are not straight lines like we reconstruct them in our models of *Caiman* and *Orobates,* and they would curve around other muscles and bones or could attach to connective tissue. This would increase or decrease the muscle length and can affect the measured muscle strains. Even the individual muscle microstructure such as differences in the pennation angle likely affects the muscle strain assessment (Lautenschlager, 2015). Nevertheless, a similar modeling approach as has been used here has been employed

to study cranial musculature and showed that this approach can lead to meaningful results, i.e., that predictions even from such simplified muscle models match empirical data well (Lautenschlager, 2015). Undoubtedly, the approach needs further testing in the context of locomotion. Again, if established, it would present a very useful technique to gain insight into the posture and gait of extinct tetrapod species.

Nevertheless, the modeling approach utilized here failed to single out one specific predicted posture or even to rule out a suite of modeled postures for *Orobates*. Indeed, none of the modeled postures did involve problematic excessive strains. This result could simply demonstrate a postural variability of *Orobates* which even exceeded that of modern *Caiman* (see above). Alternatively, this could point to limited prediction strength of the method. Potentially, prediction strength could be improved by including additional (intrinsic) limb muscles such as knee and ankle extensors, more elaborate optimization criteria, and more detailed muscle anatomy (e.g., pennation angles, variable lengths of muscles and tendons, etc.). Instantaneous muscle lever arms could further help to constrain postures as was recently attempted in a study on Nile crocodiles (Wiseman et al., 2021). In sophisticated musculo-skeletal models of vertebrate postcranial function most of these issues are taken into account and even muscle activation patterns may be predicted (e.g., recent papers by Bishop et al., 2021; Stark et al., 2021), but necessitate considerable modeling effort. A simpler approach such as the muscle strain analysis used in the current study therefore offers an alternative, for example for a first reduction of the solution space of potential postures especially in broader scaled comparative studies.

## CONCLUSION

The current study builds on previous work on the locomotion of *Orobates pabsti*, a putative stem amniote from the Permian period, by taking soft tissues into account. The proposed modeling approach of highly abstracted muscles responsible for lifting the trunk off the ground and for the generation of propulsion during walking locomotion at different simulated body heights was able to approximately predict the posture of extant *Caiman crocodilus*. This finding derived from "virtual experiments" that systematically varied body height, justified the transfer of the methodology to *Orobates* in order to gain further insight into the locomotor capabilities of this key early tetrapod. Muscle models were added to an already existing skeletal reconstruction of the holotype specimen of *Orobates*. Further, the animated locomotion stemming from a previous study was used. As in the validation experiment of *Caiman*, body height was systematically varied. While none of the simulated step cycles at different body heights resulted in the occurrence of implausible muscle strains and thus no posture could be dismissed outright, an "intermediate" posture minimized deviations from optimal muscle strains between 70 and 130% of the resting length (however, only due to a slightly better result than almost equally good results for other body heights). Body height at this "intermediate" posture is consistent with independent results from kinematic and dynamic simulations of the previous study (Nyakatura et al., 2019). Thus, our current study, albeit not narrowing posture down even more, does not contradict the hypothesized advanced locomotor capabilities of *Orobates* and strengthens previous evidence for the locomotor reconstruction of the last common ancestor of diadectids and crown amniotes. More generally and even though overall prediction strength may be weaker than comparable more sophisticated musculo-skeletal modeling approaches, the here employed methodology of simplified muscle modeling, which is relatively easy to implement, could be useful especially in comparative studies into the reconstruction of posture of extinct tetrapods.

## DATA AVAILABILITY STATEMENT

The original contributions presented in the study are included in the article/**Supplementary Material**, further inquiries can be directed to the corresponding author/s.

## ETHICS STATEMENT

The animal study was reviewed and approved by the Thüringer Landesamt für Verbraucher- und Umweltschutz (registration number: 02-008/11).

## AUTHOR CONTRIBUTIONS

JN and SL conceived of the study. OD prepared interactive animation of *Caiman crocodilus*. SL transferred models from Maya into Blender. MZ and JN reconstructed muscles, conducted the muscle strain modeling, analyzed the data, drafted figures, and prepared the manuscript draft. All authors interpreted data, and revised, read, and approved the manuscript.

## FUNDING

This study received funding from a Volkswagen Foundation grant (AZ 90222 to JN) and a Daimler and Benz Foundation grant (32-08/12 to JN). JN was also supported by the German Research Council (DFG EXC 1027, DFG EXC 2025).

## ACKNOWLEDGMENTS

We thank La Ferme aux Crocodiles (Pierrelatte, France) for making two *Caiman crocodilus* available for this study. We further thank R. Petersohn, I. Weiß, S. Clemens, and V. Allen for their contribution to the X-ray motion analysis of live *Caiman* specimens. We are indebted to J. Lauströer and A. Andikfar for their initial concept of a X-ray video collage of *Caiman*. We thank the two reviewers for their critical comments on a previous version, which greatly helped to improve the manuscript.

## SUPPLEMENTARY MATERIAL

The Supplementary Material for this article can be found online at: https://www.frontiersin.org/articles/10.3389/fevo.2021.659039/full#supplementary-material

## REFERENCES


Anderson, P. S. L., Bright, J. A., Gill, P. G., Palmer, C., and Rayfield, E. J. (2012). Models in palaeontological functional analysis. *Biol. Lett.* 8, 119–122. doi: 10.1098/rsbl.2011.0674

Arnold, P., Fischer, M. S., and Nyakatura, J. A. (2014). Soft tissue influence on ex vivo mobility in the hip of Iguana: comparison with in vivo movement and its bearing on joint motion of fossil sprawling tetrapods. *J. Anat.* 225, 31–41. doi: 10.1111/joa.12187

Ashley-Ross, M. (1994). Hindlimb kinematicas during terrestrial locomotion in a salamander (*Dicamptodon Tenebrosus*). *J. Exp. Biol.* 193, 255–283.

Ashley-Ross, M. A. (1992). The comparative myology of the thigh and crus in the salamanders *Ambystoma tigrinum* and *Dicamptodon tenebrosus*. *J. Morphol.* 211, 147–163. doi: 10.1002/jmor.1052110204

Barclay, O. (1946). The mechanics of amphibian locomotion. *J. Exp. Biol.* 23:177. doi: 10.1242/jeb.23.2.177

Bates, K. T., and Falkingham, P. L. (2012). Estimating maximum bite performance in *Tyrannosaurus* rex using multi-body dynamics. *Biol. Lett.* 8, 660–664. doi: 10.1098/rsbl.2012.0056

Berman, D. S., and Henrici, A. C. (2003). Homology of the astragalus and structure and function of the tarsus of Diadectidae. *J. Paleontol.* 77, 172–188. doi: 10.1017/S002233600004350X

Berman, D. S., Henrici, C. M. Y., Richard, A., Sumida, S. S., and Martens, T. (2004). A new Diadectid (Diadectomorpha), Orobates Pabsti, from the early Permian of central Germany. *Bull. Carnegie Mus. Nat. Hist.* 35, 1–36. doi: 10.2992/0145-9058(2004)35[1:anddop]2.0.co;2

Bishop, P. J., Cuff, A. R., and Hutchinson, J. R. (2021). How to build a dinosaur: musculoskeletal modeling and simulation of locomotor biomechanics in extinct animals. *Paleobiology* 58, 1–38. doi: 10.1017/pab.2020.46

Blob, R. W. (2001). Evolution of hindlimb posture in nonmammalian therapsids: biomechanical tests of paleontological hypotheses. *Paleobiology* 27, 14–38. doi: 10.1666/0094-8373(2001)027<0014:eohpin>2.0.co;2

Brainerd, E. L., Baier, D. B., Gatesy, S. M., Hedrick, T. L., Metzger, K. A., Gilbert, S. L., et al. (2010). X-ray reconstruction of moving morphology (XROMM): precision, accuracy and applications in comparative biomechanics research. *J. Exp. Zool. Part A Ecol. Genet. Physiol.* 313, 262–279.

Clack, J. A. (2006). The emergence of early tetrapods. *Palaeogeogr. Palaeoclimatol. Palaeoecol.* 232, 167–189. doi: 10.1016/j.palaeo.2005.07.019

Clack, J. A., and Bénéteau, A. (2012). *Gaining Ground: The Origin and Evolution of Tetrapods*, Second Edn. Bloomington: Indiana University Press

Coates, M. I., and Ruta, M. (2007). *Skeletal Changes in the Transition from Fins to Limbs*. Chicago, IL: Univ. of Chicago Press.

Cunningham, J. A., Rahman, I. A., Lautenschlager, S., Rayfield, E. J., and Donoghue, P. C. J. (2014). A virtual world of paleontology. *Trends Ecol. Evol.* 29, 347–357. doi: 10.1016/j.tree.2014.04.004

Demuth, O. E., Rayfield, E. J., and Hutchinson, J. R. (2020). 3D hindlimb joint mobility of the stem-archosaur *Euparkeria capensis* with implications for postural evolution within Archosauria. *Sci. Rep.* 10:15357. doi: 10.1038/s41598-020-70175-y

Diogo, R., Johnston, P., Molnar, J. L., and Esteve-Altava, B. (2016). Characteristic tetrapod musculoskeletal limb phenotype emerged more than 400 MYA in basal lobe-finned fishes. *Sci. Rep.* 6:37592. doi: 10.1038/srep37592

Fischer, M. S., Schilling, N., Schmidt, M., Haarhaus, D., and Witte, H. (2002). Basic limb kinematics of small therian mammals. *J. Exp. Biol.* 205, 1315–1338. doi: 10.1242/jeb.205.9.1315

Fuller, P. O., Higham, T. E., and Clark, A. J. (2011). Posture, speed, and habitat structure: three-dimensional hindlimb kinematics of two species of Padless geckos. *Zoology* 114, 104–112. doi: 10.1016/j.zool.2010.11.003

Garwood, R., and Dunlop, J. (2014). The walking dead: blender as a tool for paleontologists with a case study on extinct arachnids. *J. Paleontol.* 88, 735–746. doi: 10.1666/13-088

Gatesy, S. M. (1989). *Archosaur Neuromuscular and Locomotor Evolution*. Ph.D. thesis. Cambridge, MA: Harvard University.

Gatesy, S. M. (1991). Hind limb movements of the American alligator (*Alligator mississippiensis*) and postural grades. *J. Zool.* 224, 577–588. doi: 10.1111/j.1469-7998.1991.tb03786.x

Gatesy, S. M. (1997). An electromyographic analysis of hindlimb function in *Alligator* during terrestrial locomotion. *J. Morphol.* 234, 197–212. doi: 10.1002/(sici)1097-4687(199711)234:2<197::aid-jmor6>3.0.co;2-9

Gatesy, S. M., Baier, D. B., Jenkins, F. A., and Dial, K. P. (2010). Scientific rotoscoping: a morphology-based method of 3-D motion analysis and visualization. *J. Exp. Zool. A Ecol. Genet. Physiol.* 313, 244–261. doi: 10.1002/jez.588

Hutchinson, J. R. (2001). The evolution of pelvic osteology and soft tissues on the line to extant birds (Neornithes). *Zool. J. Linn. Soc.* 131, 123–168. doi: 10.1006/zjls.2000.0254

Hutchinson, J. R. (2012). On the inference of function from structure using biomechanical modelling and simulation of extinct organisms. *Biol. Lett.* 8, 115–118. doi: 10.1098/rsbl.2011.0399

Hutchinson, J. R., and Gatesy, S. M. (2000). Adductors, abductors, and the evolution of archosaur locomotion. *Paleobiology* 26, 734–751. doi: 10.1666/0094-8373(2000)026<0734:aaateo>2.0.co;2

Karakasiliotis, K., Thandiackal, R., Melo, K., Horvat, T., Mahabadi, N. K., Tsitkov, S., et al. (2016). From cineradiography to biorobots: an approach for designing robots to emulate and study animal locomotion. *J. R. Soc. Interface* 13:20151089. doi: 10.1098/rsif.2015.1089

Kawano, S. M., and Blob, R. W. (2013). Propulsive forces of mudskipper fins and salamander limbs during terrestrial locomotion: implications for the invasion of land. *Integr. Comp. Biol.* 53, 283–294. doi: 10.1093/icb/ict051

Koolstra, J. H., and van Eijden, T. M. (1995). Biomechanical analysis of jaw-closing movements. *J. Dent. Res.* 74, 1564–1570. doi: 10.1177/00220345950740091001

Laurin, M., and Reisz, R. R. (1995). A reevaluation of early amniote phylogeny. *Zool. J. Linn. Soc.* 113, 165–223. doi: 10.1111/j.1096-3642.1995.tb00932.x

Laurin, M., and Reisz, R. R. (1997). "A new perspective on tetrapod phylogeny," in *Amniote Origins: Completing the Transition to Land*, eds S. Sumida and K. Martin (San Diego, CA: Academic Press), 9–59. doi: 10.1016/b978-012676460-4/50003-2

Lautenschlager, S. (2015). Estimating cranial musculoskeletal constraints in theropod dinosaurs. *R. Soc. Open Sci.* 2:150495. doi: 10.1098/rsos.150495

Lautenschlager, S. (2016). Digital reconstruction of soft-tissue structures in fossils. *Paleontol. Soc. Pap.* 22, 101–117. doi: 10.1017/scs.2017.10

Lautenschlager, S. (2020). Multibody dynamics analysis (MDA) as a numerical modelling tool to reconstruct the function and palaeobiology of extinct organisms. *Palaeontology* 63, 703–715. doi: 10.1111/pala.12501

Lee, M. S. Y., and Spencer, P. S. (1997). "Crown-Clades, key characters and taxonomic stability: when is an amniote not an amniote?," in *Amiote Origins - Completing the Transition to Land*, eds S. S. Sumida and K. L. Martin (San Diego, CA: Academic Press)

Manafzadeh, A. R., and Padian, K. (2018). ROM mapping of ligamentous constraints on avian hip mobility: implications for extinct ornithodirans. *Proc. R. Soc. B Biol. Sci.* 285:20180727. doi: 10.1098/rspb.2018.0727

Marjanović, D., and Laurin, M. (2019). Phylogeny of Paleozoic limbed vertebrates reassessed through revision and expansion of the largest published relevant data matrix. *PeerJ* 6:e5565. doi: 10.7717/peerj.5565

Martin, K., and Sumida, S. S. (1997). *Amniote Origins: Completing the Transition to Land*. San Diego, CA: Academic Press

Molnar, J. L., Diogo, R., Hutchinson, J. R., and Pierce, S. E. (2020). Evolution of hindlimb muscle anatomy across the tetrapod water-to-land transition, including comparisons with forelimb anatomy. *Anat. Rec. (Hoboken)* 303, 218–234. doi: 10.1002/ar.23997

Nyakatura, J. A. (2017). "Description, experiment, and model. reading traces in paleobiological research exemplified by a morpho-functional analysis," in *Traces*, ed. B. Bock von Wülfingen (Berlin: De Gruyter), 15–28.

Nyakatura, J. A. (2019). Making use of a track-trackmaker association: locomotor inference of an early amniote with help of "fossilized behavior". *Hallesches Jahrbuch Geowissenschaften Beiheft* 46, 67–75.

Nyakatura, J. A., Allen, V. R., Lauströer, J., Andikfar, A., Danczak, M., Ullrich, H.-J., et al. (2015). A three-dimensional skeletal reconstruction of the stem amniote *Orobates pabsti* (Diadectidae): analyses of body mass, centre of mass position, and joint mobility. *PLoS One* 10:e0137284. doi: 10.1371/journal.pone.0137284

Nyakatura, J. A., and Demuth, O. E. (2019). "Modellieren. Virtuelle Experimente zur funktionellen Morphologie," in *Experimentieren: Einblicke in Praktiken und Versuchsaufbauten zwischen Wissenschaft und Gestaltung*, eds S. Marguin, H. Rabe, W. Schäffner, and F. Schmidgall (Bielefeld: Transcript Verlag)

Nyakatura, J. A., Andrada, E., Curth, S., and Fischer, M. S. (2014). Bridging "Romer's Gap": limb mechanics of an extant belly-dragging lizard inform debate on tetrapod locomotion during the early carboniferous. *Evol. Biol.* 41, 175–190. doi: 10.1007/s11692-013-9266-z

Nyakatura, J. A., Melo, K., Horvat, T., Karakasiliotis, K., Allen, V. R., Andikfar, A., et al. (2019). Reverse-engineering the locomotion of a stem amniote. *Nature* 565, 351–355. doi: 10.1038/s41586-018-0851-2

Otero, A., Gallina, P. A., and Herrera, Y. (2010). Pelvic musculature and function of *Caiman latirostris*. *Herpetol. J.* 20, 173–184.

Reilly, S. M., Willey, J. S., Biknevicius, A. R., and Blob, R. W. (2005). Hindlimb function in the alligator: integrating movements, motor patterns, ground reaction forces and bone strain of terrestrial locomotion. *J. Exp. Biol.* 208, 993–1009. doi: 10.1242/jeb.01473

Reisz, R. R. (1997). The origin and early evolutionary history of amniotes. *Trends Ecol. Evol.* 12, 218–222. doi: 10.1016/S0169-5347(97)01060-4

Riskin, D. K., Kendall, C. J., and Hermanson, J. W. (2016). The crouching of the shrew: mechanical consequences of limb posture in small mammals. *PeerJ* 4:e2131. doi: 10.7717/peerj.2131

Romer, A. S. (1922). The locomotor apparatus of certain primitive and mammal-like reptiles. *Bull. AMNH* 46, article 10, 517–606.

Russell, A. P., and Bels, V. (2001). Biomechanics and kinematics of limb-based locomotion in lizards: review, synthesis and prospectus. *Comp. Biochem. Physiol. Part A Mol. Integr. Physiol.* 131, 89–112. doi: 10.1016/s1095-6433(01)00469-x

Schilling, N., Fischbein, T., Yang, E. P., and Carrier, D. R. (2009). Function of the extrinsic hindlimb muscles in trotting dogs. *J. Exp. Biol.* 212, 1036–1052. doi: 10.1242/jeb.020255

Sherwood, L., Klandorf, H., and Yancey, P. H. (2013). *Animal Physiology: From Genes to Organisms*. Pacific Grove, CA: Calif. Brooks/Cole.

Snively, E., Cotton, J. R., Ridgely, R., and Witmer, L. M. (2013). Multibody dynamics model of head and neck function in *Allosaurus* (Dinosauria, Theropoda). *Palaeontol. Electron.* 16:11A.

Stark, H., Fischer, M. S., Hunt, A., Young, F., Quinn, R., and Andrada, E. (2021). A three-dimensional musculoskeletal model of the dog. *Sci. Rep.* 11:11335.

Sullivan, C. S. (2007). *Function and Evolution of the Hind Limb in Triassic Archosaurian Reptiles.* Ph.D. thesis. Cambridge, MA: Harvard University.

Sumida, S. S., and Modesto, S. (2001). A phylogenetic perspective on locomotory strategies in early amniotes. *Integr. Comp. Biol.* 41, 586–597. doi: 10.1093/icb/41.3.586

Sutton, M. D. (2008). Tomographic techniques for the study of exceptionally preserved fossils. *Proc. Biol. Sci.* 275, 1587–1593. doi: 10.1098/rspb.2008.0263

Voigt, S., Berman, D. S., and Henrici, A. C. (2007). First well-established track-trackmaker association of paleozoic tetrapods based on *Ichniotherium* trackways and diadectid skeletons from the Lower Permian of Germany. *J. Vertebr. Paleontol.* 27, 553–570.

Watt, A., and Watt, M. (1992). *Advanced Animation and Rendering Techniques: Theory and Practice*. New York, NY: ACM Press

Wiseman, A. L. A., Bishop, P. J., Demuth, O. E., Cuff, A. R., Michel, K. B., and Hutchinson, J. R. (2021). Musculoskeletal modelling of the Nile crocodile (*Crocodylus niloticus*) hindlimb: effects of limb posture on leverage during terrestrial locomotion. *J. Anat. JOA* 239, 424–444. doi: 10.1111/joa.13431

Witmer, L. M. (1995). "The extant phylogenetic bracket and the importance of reconstruction soft tissues in fossils," in *Functional Morphology in Vertebrate Paleontology*, ed. J. J. Thomason (Cambridge: Cambridge University Press) 19–33.

**Conflict of Interest:** The authors declare that the research was conducted in the absence of any commercial or financial relationships that could be construed as a potential conflict of interest.

**Publisher's Note:** All claims expressed in this article are solely those of the authors and do not necessarily represent those of their affiliated organizations, or those of the publisher, the editors and the reviewers. Any product that may be evaluated in this article, or claim that may be made by its manufacturer, is not guaranteed or endorsed by the publisher.